MODEL CORRECTED LOW RANK PTYCHOGRAPHY

Gauri Jagatap, Zhengyu Chen, Chinmay Hegde and Namrata Vaswani

Iowa State University

ABSTRACT

In this paper, we introduce a novel algorithmic framework for sub-diffractive super-resolution imaging of dynamic, time-varying targets. We extend recent works in low rank Fourier ptychographic imaging, to incorporate *model-correction* schemes, which correct for errors propagated due to inaccuracies in fitting an exact low rank model to the target video acquired. Through our algorithm, we are able to demonstrate superior reconstruction quality of video from phaseless Fourier ptychographic measurements, at low sample complexities, as compared to conventional ptychographic setups.

***Index Terms*—** Fourier, ptychography, phase retrieval, low-rank, microscopic imaging.

1. INTRODUCTION

1.1. Motivation

The classical phase retrieval problem arises in standard Fourier imaging practices, where an n-dimensional discrete-time signal needs to be reconstructed from (noisy) observations of magnitudes of discrete Fourier transform (DFT) coefficients. A generalized version of phase retrieval studies a similar reconstruction problem with a class of linear measurement operators, constructed by sampling vectors from certain families of multivariate probability distributions, and several theoretically sound algorithms have been developed in this direction [1, 2, 3, 4, 5].

Applications of phase retrieval algorithms include imaging applications such as X-ray crystallography and biomedical imaging [6, 7, 8], including *Fourier ptychography*, which is a image super-resolution technique for diffraction-blurred *microscopic images*. The imaging setup consists of a programmable coherent illumination source coupled with two lenses, to capture the target scene. This is followed by an image reconstruction scheme using phase retrieval algorithms, to super-resolve images beyond the diffraction-limit of the objective lens in a microscope. The acquisition setup can consist of either spatially translating a single camera aperture [9], or can constitute an array of fixed cameras, each of which captures different portions of the Fourier spectrum of the desired high-resolution image [10]. Recently, Holloway et al. have demonstrated similar results in the context of *long-distance* sub-diffraction imaging [11], which is guided by similar optical principles.

The sample complexity, in terms of the number of observations required for a single image frame, can be particularly high ($\Omega(n)$), for Fourier ptychographic measurement setups. To alleviate these issues, Fourier ptychography for *static* scenes that obey intra-frame models on sparsity and/or structured sparsity have been recently studied [12]. Further, we consider the challenge of capturing a *dynamic* scene involving a moving target using the ptychographic setup. Then, for a video sequence with q images each with resolution n, the number of observations must be at least $\Omega(nq)$, without using any structural prior assumptions, which is computationally challenging.

1.2. Our contributions

In this paper, we introduce a new algorithmic framework for imaging of dynamic, time-varying targets, under the Fourier ptychographic measurement setup. This setup was first introduced in [13], and is based on the idea that if the dynamics of the scene are sufficiently slow, then the underlying video can be well-modeled by a *low-rank matrix*. This modeling assumption has been successfully employed in a variety of video acquisition, compression, and segmentation applications [14, 15, 16, 17, 18].

Specifically, we are given a video volume $\boldsymbol{X} \in \mathbb{R}^{n \times q}$, with each column $\boldsymbol{x}_k \in \mathbb{R}^n$ representing a vectorized image frame, q such consecutive frames. In this case, $\boldsymbol{X}$ is *approximately* rank-r, with $r \ll \min(n, q)$.

In this paper, we demonstrate how we can recover high resolution, approximately low-rank structured videos/ We also compare the reconstruction quality to traditional frame-by-frame image reconstruction methods, using fewer measurements than previously demonstrated in a similar imaging setup [13]. To this end, we propose a novel *model-correction* scheme, which adjusts for any errors in reconstruction, that may have propagated due to (i) incorrect selection of the rank parameter r or (ii) data is not exactly, but approximately low rank. We utlize "under-sampling" strategies that were originally devised in [13, 12], which we demonstrate, can considerably reduce the sample complexity of low rank video Fourier ptychography. We further extend the merits of our previous work [13] on Low Rank Fourier Ptychography (LRPtych) with a new reconstruction algorithm which fully

exploits the underlying low-rank structure of the target video sequence, and also additionally allows for a modeling error correction. Moreover, we present a number of simulation experiments, which justify the superior properties of our new algorithm.

Our algorithm builds upon techniques introduced in our recent work on low rank phase retrieval under the Gaussian, coded-diffraction patterned (CDP) [19], and Fourier Ptychographic [13] measurement setups . While [13] was specifically tailored for the Fourier ptychographic framework under a strict low rank assumption, such an assumption can be unrealistic for real videos. We therefore expand the utility of LRPtych [13], for real videos, where the low-rank assumption may be easily violated. To this end, we propose our new algorithm, that we call Modified Low Rank Ptychography, or *MLRPtych*. Our new reconstruction algorithm MLRPtych, involves a non-convex, alternating minimization based estimation procedure. The advantages of the overall algorithmic setup are *three-fold*:

1. We utilize the novel initialization strategy from [13] which improves upon standard initialization schemes proposed in [11] to yield a good initial estimate for our iterative image reconstruction procedure,
2. We demonstrate a significantly improved recovery for under-sampled measurements, a model which is in general, ill-posed. We propose a modeling error correction methodology, to "undo" any errors that may have propagated due to the strict low rankness assumption. This contribution is significant, as it qualifies a wide variety of videos as suitable for our recovery strategy, not just videos with strict underlying low-rankness. This modeling-error correction improves the performance of LRPtych greatly, which otherwise does not match up to IERA [11] (a frame-by-frame reconstruction method), when full or nearly full data is available. MLRPtych however outperforms both LRPtych and IERA under all under-sampling settings.
3. Our two under-sampling strategies, which have been borrowed from [13, 12] *do not require* the apparatus of the pre-existing setup in conventional Fourier ptychography [11], to be changed by much; in one such strategy, one would simply need to turn off a fraction of the cameras constituting the camera array.

We explain these three stages in detail in the Section 3. We experimentally demonstrate that our new modified reconstruction algorithm MLRPtych, compares favorably in terms of sample complexity as compared to the original algorithm LRPtych [13], as well as existing "single-frame" methods, such as the Iterative Error Reduction Algorithm (IERA) [11], which does not utilize the low rank nature of the video acquired. This paper focuses on Fourier ptychographic acquisition of dynamic scenes that are approximately but not exactly low-rank. The assumption of an "approximate low-rankness", reduces sample complexity, additionally, the model-correction strategy, rectifies for errors that must have propagated due to inaccuracies in low-rank approximation.

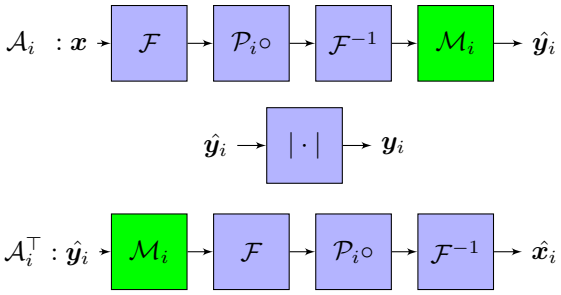

Fig. 1. Sequence of operations defined by $\mathcal{A}_i$. Here the green box indicates the extra sub-sampling step and $i = [N]$ denotes the camera index.

2. PROBLEM SETUP

2.1. Optical setting

The sub-sampled Fourier ptychographic measurement procedure, based on the setup of [13, 12] is described in Fig. 1. The field of illumination at the aperture plane, under Fraunhofer approximation, can be written as the Fourier transform ($\mathcal{F}(\cdot)$) of the image at the object plane ($\boldsymbol{x}$). Light then passes through an array of *overlapping* camera lenses, whose apertures individually are limited in size ($\mathcal{P}_i(\cdot)$, i spans index of the cameras), but the collective array yields a large synthetic aperture. The light then propagates to the plane of image sensor, and this process can be represented by an inverse Fourier transform operation ($\mathcal{F}^{-1}(\cdot)$). The setup so far is similar to that in [11]. At this point, we introduce a *sub-sampling* stage ($\mathcal{M}_i(\cdot)$), which effectively discards some of the pixels captured by the sensing apparatus. As only the magnitude of a light field can be recorded by the image sensors, all the phase information gets discarded ($\boldsymbol{y}$).

2.2. Mathematical description

We now describe the mathematical formulation of the setup described above. We consider a high resolution video frame at time instant k, denoted by $\boldsymbol{x}_k$. We define the video matrix $\boldsymbol{X}$, composed of frames $\boldsymbol{x}_k$ for $k \in [q] := \{1, \dots q\}$:

$$\boldsymbol{X} := [\boldsymbol{x}_1, \boldsymbol{x}_2, \dots, \boldsymbol{x}_q],\ \boldsymbol{X} \in \mathbb{R}^{n \times q}$$

We assume that the frames of video are changing sufficiently slowly, and hence the rank of matrix $\boldsymbol{X}$ is no greater than r, with $r \ll \min(n, q)$. For each video frame $\boldsymbol{x}_k$, the ptychographic measurements $\boldsymbol{y}_{i,k} \in \mathbb{R}^n$ corresponding to the i^{th} camera location take the form:

$$\boldsymbol{y}_{i,k} = |\mathcal{A}_{i,k}(\boldsymbol{x}_k)|, \quad \boldsymbol{y}_k = [\boldsymbol{y}_{1,k}\ \boldsymbol{y}_{2,k} \dots \boldsymbol{y}_{N,k}]^\top \in \mathbb{R}^{N \times n}.$$

Here, we introduce the operator $\mathcal{A}_{i,k}$ to represent overall ptychographic measure operation, where the index $i \in [N]$ corresponds to different camera positions, and the index $k = [q]$ indicates the time stamp. In terms of various stages of the

acquisition process, the operator $\mathcal{A}_{i,k}$ can be expressed as:

$$\mathcal{A}_{i,k}(\cdot) = \mathcal{M}_{i,k}\mathcal{F}^{-1}\mathcal{P}_i \circ \mathcal{F}(\cdot),$$

where $\mathcal{M}_{i,k}$ represents the subsampling mask corresponding to i^{th} camera and k^{th} frame. The subsampling mask itself, can follow two different configurations: (i) random pixel subsampling: $\mathcal{M}_{i,k} : \mathbb{R}^n \rightarrow \mathbb{R}^n$ is such that the effective operation choses pixels of its argument uniform randomly and applies a mask of 0s and 1s based on the under-sampling ratio desired, (ii) random camera sub-sampling: for a fixed frame k, the camera position i is chosen uniform randomly, and *all* of the pixels corresponding to the i^{th} camera are assigned 0s or 1s, similar to the measurement setup in [13, 12].

Under this assumption, we first recover the low rank solution $\tilde{\boldsymbol{X}}$ to the non-convex optimization problem:

$$\tilde{\boldsymbol{X}} := \underset{\boldsymbol{X}}{\operatorname{argmin}} \sum_{k=1}^{q}\sum_{i=1}^{N} \|\boldsymbol{y}_{i,k} - |\mathcal{A}_{i,k}(\boldsymbol{x}_k)|\|_2^2, \quad (1)$$
$$\text{s.t.} \quad \operatorname{rank}(\boldsymbol{X}) = r.$$

In the second stage, we invoke the *model correction* subroutine, to fix any errors that may have propagated due to inaccuracy in selecting the rank r, from the standard LRPtych algorithm. This stage constitutes the modification, and is the main element on the Modified Low Rank Ptychography (or MLRPtych) algorithm. Mathematically, this represents the following optimization problem:

$$\hat{\boldsymbol{X}} := \tilde{\boldsymbol{X}} + \underset{\boldsymbol{E}}{\operatorname{argmin}} \sum_{k=1}^{q}\sum_{i=1}^{N} \|\boldsymbol{y}_{i,k} - |\mathcal{A}_{i,k}(\boldsymbol{x}_k + \boldsymbol{e}_k)|\|_2^2 \quad (2)$$

where $\boldsymbol{E} = [\boldsymbol{e_1}, \boldsymbol{e_2}, \dots \boldsymbol{e_q}]$, $E \in \mathbb{R}^{n\times q}$ is the modeling error.

3. ALGORITHM

To solve the two stage problem in Equations 1 and 2, we deploy the Modified Low Rank Ptychopgraphy (MLRPtych) algorithm, modeled on the base algorithm from [13]. It consists of three different stages: (i) the initialization, (ii) an alternating minimization based low rank matrix recovery, and finally (iii) a modeling error correction procedure which corrects any error in the recovered video that arises due to inaccurate low-rank estimation of the video. This algorithm is described in Alg.1.

3.1. Initialization

In recent phase-retrieval literature there has been significant attention on designing initialization schemes which benefit the phase recovery strategy by (i) reducing the number of iterations required for convergence (ii) ensuring convergence to the true solution. We utilize the novel initialization strategy from [13], which can be found in lines 1-7 of Alg. 1.

Algorithm 1 Modified Low Rank Ptychography (MLRPtych)

(Initialization)
1: **Input:** $\boldsymbol{y}_k, \mathcal{A}_{i,k}, r$
2: **for** $k = 1, 2, \dots, q$ **do**
3: $\quad \boldsymbol{x}_k^0 \leftarrow \sqrt{\frac{1}{L}\sum_{i=1}^{L} \boldsymbol{y_{i,k}}^2}$
4: **end for**
5: $[\boldsymbol{U}^0, \boldsymbol{S}^0, \boldsymbol{V}^0] \leftarrow ReducedSVD((\boldsymbol{X}^0), r)$
6: **for** $k = 1, 2, \dots, q$ **do**
7: $\quad \boldsymbol{b}_k^0 \leftarrow (\boldsymbol{S}^0\boldsymbol{V}^{0\top})_k$
8: **end for**
(Low-rank matrix recovery stage)
9: **for** $t = 1, 2, \dots, T$ **do**
10: $\quad$ a) $\boldsymbol{C}_k^t \leftarrow \operatorname{diag}(phase(\mathcal{A}_k(\boldsymbol{U}^{t-1}\boldsymbol{b}_k^{t-1}))), k = [q]$
11: $\quad$ b) $\boldsymbol{U}^{tmp} \leftarrow \operatorname{argmin}_{\tilde{U}} \sum_k \left\|\boldsymbol{C}_k^t\boldsymbol{y}_k - \mathcal{A}_k(\tilde{\boldsymbol{U}}\boldsymbol{b}_k^{t-1})\right\|^2$
12: $\quad$ c) $\boldsymbol{U}^t \leftarrow QR(\boldsymbol{U}^{tmp})$
13: $\quad$ d) $\boldsymbol{b}_k^t \leftarrow \operatorname{argmin}_{\tilde{\boldsymbol{b}}_k} \left\|\boldsymbol{C}_k^t\boldsymbol{y}_k - \mathcal{A}_k(\boldsymbol{U}^t\tilde{\boldsymbol{b}}_k)\right\|^2, k = [q]$
14: **end for**
(Modeling-error correction stage)
15: **for** $k = 1, 2, \dots, q$ **do**
16: $\quad \tilde{\boldsymbol{x}_k}^0 = \boldsymbol{U}^T\boldsymbol{b}_k^T$
17: $\quad \hat{\boldsymbol{x}_k^0} = \tilde{\boldsymbol{x}_k}^0 + \boldsymbol{e}_k^0$
18: $\quad$ **for** $t = 1, 2, \dots, T'$ **do**
19: $\quad\quad$ e) $\boldsymbol{C}_k^t \leftarrow \operatorname{diag}(phase(\mathcal{A}_k(\hat{\boldsymbol{x}_k}^t)))$
20: $\quad\quad$ f) $\boldsymbol{e}_k^t \leftarrow \operatorname{argmin}_{\boldsymbol{e}}(\left\|\boldsymbol{C}_k^t\boldsymbol{y}_k - \mathcal{A}_k(\hat{\boldsymbol{x}_k}^t + \boldsymbol{e})\right\|_2^2 + \tau\|\boldsymbol{e}\|_2^2)$
21: $\quad\quad$ g) $\hat{\boldsymbol{x}_k}^{t+1} = \hat{\boldsymbol{x}_k}^t + \boldsymbol{e}_k^t$
22: $\quad$ **end for**
23: **end for**
24: **Output:** $\boldsymbol{X}^* = \hat{\boldsymbol{X}}^{T'+1}$

3.2. Alternate recovery of phase and low rank matrix

Inspired by early works in phase retrieval literature and our base papers[19, 13], we adapt the Low Rank Phase Retrieval (LRPR) algorithm for the Fourier ptychographic setup [13]. This stage (lines 8-14 of Alg. 1) consists of alternatingly (i) estimating the phase (step (a) of Alg. 1) and (ii) estimating the low rank matrix (step (d) of Alg. 1).

3.3. Modeling-error correction

Finally, we proceed to the modeling error correction stage (lines 15-20 of Alg.1). In Alg. 1, $\tilde{\boldsymbol{X}}^0$ is the estimate of a low rank video from the LRPtych stage. However, for most real videos, the low-rank model assumption, is often inconsistent, and cannot describe the video characteristics precisely. Here, we introduce new notation, to demarcate the real video $\boldsymbol{X}^*$. In the modeling error correction stage, we produce $\hat{\boldsymbol{X}}^{t'} \rightarrow \boldsymbol{X}^*$. We initialize this stage as $\hat{\boldsymbol{X}}^0 = \tilde{\boldsymbol{X}}^0 + \boldsymbol{e}^0$ where $\tilde{\boldsymbol{X}}^0$ is the output from the previous stage, and $\boldsymbol{e}^0 = \boldsymbol{0}$ initializes the model error on real videos. From line 13 to 15, we use an alternative minimization method to estimate this model error, by alternatively updating $\boldsymbol{C}$ (step (e) of Alg. 1) and $\boldsymbol{E}$ (step (f), and subsequently step (g) of Alg. 1, $\hat{\boldsymbol{X}}$). We impose an

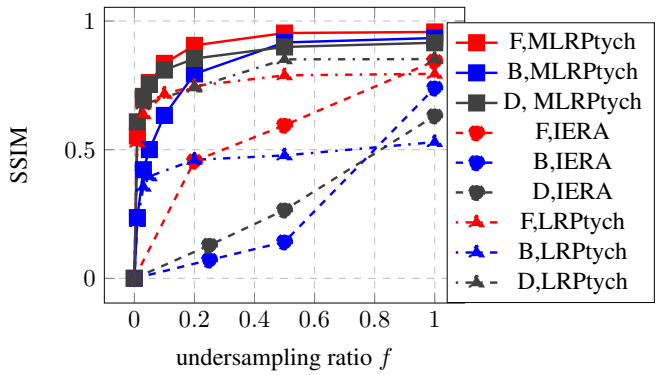

Fig. 2. Comparison of algorithms for ptychography using random pixel under-sampling.

ℓ_2 regularization on $\boldsymbol{e}_k$ to ensure that the error term is minimized. In the next section we describe some experimental results based on our MLRPtych algorithm.

4. EXPERIMENTAL RESULTS

We apply Alg. 1 for two different patterns of under-sampling. The settings used for this experiment are as follows: the data is sized as $180 \times 180 \times q$, where q varies for different videos: $q = 112$ for "Bacteria" (B) video, $q = 148$ for "Sleeping-Dog" (D) video, $q = 140$ for "Fish" (F) video. The aperture diameter of each camera considered is 40 pixels, overlap between consecutive cameras is of factor 0.48 and number of cameras in the camera array is 81 (9×9). We run lines 8-13 of MLR-Ptych algorithm for 5 iterations ($T = 5$) and 10 iterations of lines 16-19 ($T' = 10$). We run IERA for 250 outer iterations. In addition, we run original LR-Ptych algorithm (lines 8-13 of Alg. 1) for 5 iterations, as a comparison. The rank considered for all videos for is $r = 20$.

In the first set of experiments (refer Fig. 2), we consider random pixel under-sampling $\mathcal{M}_{i,k}$, where a fraction of pixels are "on" and are picked uniform randomly, according to the required sub-sampling ratio. In Fig. 3, we provide a visual comparison between the three algorithms (MLRPtych, IERA, LRPtych) that we tested in the experiment, for a fixed frame of "fish" (F) video.

In the second set of experiments (refer Fig. 4), we consider a simpler and more feasible under-sampling strategy $\mathcal{M}_{i,k}$ of turning a fraction of cameras from the camera array "on". We see similar trends of improved performance of MLRPtych w.r.t. IERA and LRPtych, in terms of SSIM, in both sets of experiments. It is also interesting to note that even under the scenario where we consider all measurements ($f = 1$), we see an improved recovery for the MLRPtych algorithm w.r.t. IERA. A visual comparison of the performance of both algorithms on "Bacteria" (B) video can be seen in 5.

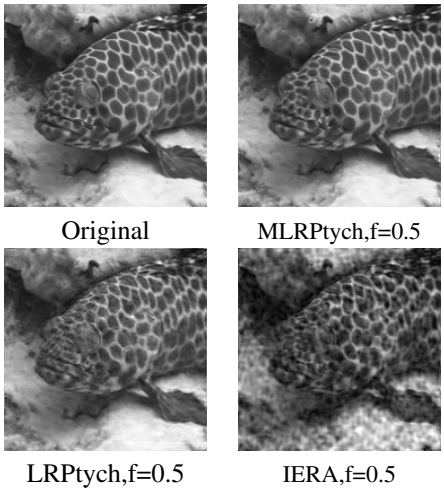

Fig. 3. Visual comparison of algorithms for ptychography using random pixel under-sampling ratio f.

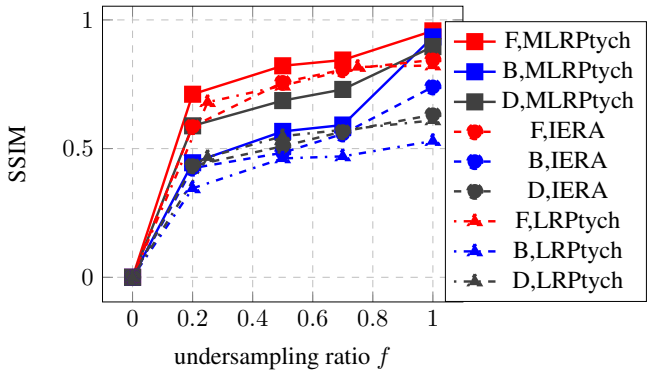

Fig. 4. Comparison of algorithms for ptychography on random camera under-sampling.

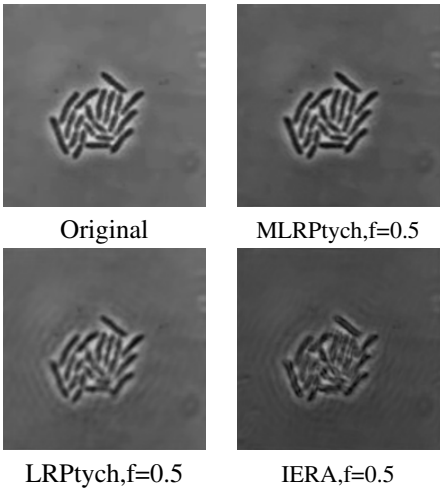

Fig. 5. Visual comparison of algorithms for ptychography using random camera under-sampling ratio f.

5. CONCLUSIONS

A model-correction strategy largely benefits the low rank Fourier ptychographic image reconstruction procedure. Significant improvements were noted, in terms of SSIM, implying better quality reconstructions, at lower sampling rates, hence extending the efficacy of our algorithmic framework for real video applications.

6. REFERENCES

[1] E. Candes, T. Strohmer, and V. Voroninski, "Phaselift: Exact and stable signal recovery from magnitude measurements via convex programming," *Communications on Pure and Applied Mathematics*, vol. 66, no. 8, pp. 1241–1274, 2013.

[2] E. Candes, X. Li, and M. Soltanolkotabi, "Phase retrieval via wirtinger flow: Theory and algorithms," *IEEE Transactions on Information Theory*, vol. 61, no. 4, pp. 1985–2007, 2015.

[3] Y. Chen and E. Candes, "Solving random quadratic systems of equations is nearly as easy as solving linear systems," in *Advances in Neural Information Processing Systems*, 2015, pp. 739–747.

[4] P. Netrapalli, P. Jain, and S. Sanghavi, "Phase retrieval using alternating minimization," in *Advances in Neural Information Processing Systems*, 2013, pp. 2796–2804.

[5] G. Wang, G. Giannakis, and Y. C. Eldar, "Solving systems of random quadratic equations via truncated amplitude flow," *IEEE Transactions on Information Theory*, 2017.

[6] Y. Shechtman, Y. C. Eldar, O. Cohen, H. N. Chapman, J. Miao, and M. Segev, "Phase retrieval with application to optical imaging: a contemporary overview," *IEEE signal processing magazine*, vol. 32, no. 3, pp. 87–109, 2015.

[7] R. Millane, "Phase retrieval in crystallography and optics," *JOSA A*, vol. 7, no. 3, pp. 394–411, 1990.

[8] A. Maiden and J. Rodenburg, "An improved ptychographical phase retrieval algorithm for diffractive imaging," *Ultramicroscopy*, vol. 109, no. 10, pp. 1256–1262, 2009.

[9] S. Dong, R. Horstmeyer, R. Shiradkar, K. Guo, X. Ou, Z. Bian, H. Xin, and G. Zheng, "Aperture-scanning fourier ptychography for 3d refocusing and super-resolution macroscopic imaging," *Optics express*, vol. 22, no. 11, pp. 13586–13599, 2014.

[10] G. Zheng, R. Horstmeyer, and C. Yang, "Wide-field, high-resolution fourier ptychographic microscopy," *Nature photonics*, vol. 7, no. 9, pp. 739–745, 2013.

[11] J. Holloway, M. S. Asif, M. K. Sharma, N. Matsuda, R. Horstmeyer, O. Cossairt, and A. Veeraraghavan, "Toward long-distance subdiffraction imaging using coherent camera arrays," *IEEE Transactions on Computational Imaging*, vol. 2, no. 3, pp. 251–265, 2016.

[12] G. Jagatap, Z. Chen, C. Hegde, and N. Vaswani, "Sub-diffraction imaging using fourier ptychography and structured sparsity," *to appear in* Proc. IEEE Int. Conf. Acoust., Speech, and Sig. Proc. (ICASSP), 2018.

[13] Z. Chen, G. Jagatap, S. Nayer, C. Hegde, and N. Vaswani, "Low rank fourier ptychography," *to appear in* Proc. IEEE Int. Conf. Acoust., Speech, and Sig. Proc. (ICASSP), 2018.

[14] P. Jain, P. Netrapalli, and S. Sanghavi, "Low-rank matrix completion using alternating minimization," in *Proceedings of the forty-fifth annual ACM symposium on Theory of computing*. ACM, 2013, pp. 665–674.

[15] E. Candès and B. Recht, "Exact matrix completion via convex optimization," *Foundations of Computational mathematics*, vol. 9, no. 6, pp. 717, 2009.

[16] J. Wright, A. Ganesh, S. Rao, Y. Peng, and Y. Ma, "Robust principal component analysis: Exact recovery of corrupted low-rank matrices via convex optimization," in *Advances in neural information processing systems*, 2009, pp. 2080–2088.

[17] S. Oymak, A. Jalali, M. Fazel, Y. C. Eldar, and B. Hassibi, "Simultaneously structured models with application to sparse and low-rank matrices," *IEEE Transactions on Information Theory*, vol. 61, no. 5, pp. 2886–2908, 2015.

[18] Y. C. Eldar, D. Needell, and Y. Plan, "Uniqueness conditions for low-rank matrix recovery," *Applied and Computational Harmonic Analysis*, vol. 33, no. 2, pp. 309–314, 2012.

[19] N. Vaswani, S. Nayer, and Y. C. Eldar, "Low-rank phase retrieval," *IEEE Transactions on Signal Processing*, vol. 65, no. 15, pp. 4059–4074, 2016.